

The rigid body and the pendulum revisited \star

Manuel de la Cruz, Néstor Gaspar, Román Linares

*Departamento de Física, Universidad Autónoma Metropolitana Iztapalapa,
San Rafael Atlixco 186, C.P. 09340, México City, México.*

Abstract

In this paper we revisit the construction by which the $SL(2, \mathbb{R})$ symmetry of the Euler equations allows to obtain the simple pendulum from the rigid body. We begin reviewing the original relation found by Holm and Marsden in which, starting from the two Casimir functions of the extended rigid body with Lie algebra $ISO(2)$ and introducing a proper momentum map, it is possible to obtain both the Hamiltonian and equations of motion of the pendulum. Important in this construction is the fact that both Casimirs have the geometry of an elliptic cylinder. By considering the whole $SL(2, \mathbb{R})$ symmetry group, in this contribution we give all possible combinations of the Casimir functions and the corresponding momentum maps that produce the simple pendulum, showing that this system can also appear when the geometry of one of the Casimirs is given by a hyperbolic cylinder and the another one by an elliptic cylinder. As a result we show that from the extended rigid body with Lie algebra $ISO(1, 1)$, it is possible to obtain the pendulum but only in circulating movement. Finally, as a by product of our analysis we provide the momentum maps that give origin to the pendulum with an imaginary time. Our discussion covers both the algebraic and the geometric point of view.

Keywords: Extended rigid body; Pendulum; Nambu dynamics;

bi-Hamiltonian systems; Lie-Poisson structures

2010 MSC: 00-01, 99-00

1. Introduction

The simple pendulum and the torque free rigid body are two well understood physical systems in both classical and quantum mechanics. The first systematic study of the pendulum is attributed to Galileo Galilei around 1602 and its dynamical description culminated with the development of the elliptic functions by Abel [1] and Jacobi [2, 3], which turn out to be the analytical solutions to the equation of motion of the pendulum (for a review of elliptic functions see for instance [4, 5, 6, 7, 8, 9] and [10, 11, 12] for the solutions of the pendulum). The quantization of the pendulum is based on the equivalence between the Schrödinger equation and the Mathieu differential equation, result developed originally by Condon in 1928 [13] and source of subsequent analysis of different aspects of the quantum system [14, 15]. On the other hand in 1758 Euler showed that the equations of motion that describe the rotation of a rigid body form a vectorial quasilinear first-order ordinary differential equations set [16]. A geometric construction of the solution was given later on by Poinsot [17] and analytically these solutions are given, as for the simple pendulum, by elliptic functions (see for instance [18, 19, 20, 21] and references therein). The quantization of the problem was attacked first by Kramers and Ittmann [22] and since then many authors have contributed to understand deeper many aspects of the problem [23, 24, 25, 26, 27, 28, 29, 30].

Despite the old age of these problems, from time to time there are some new physical aspects uncovered about these systems that contribute to our knowledge and understanding of physics in general. The list is long and here we point out just four examples: i) In 1973 Y. Nambu, taking the Liouville theorem as a guiding principle, proposed a generalization of the classical Hamiltonian dynamics by supersede the usual two dimensional phase space with a n -dimensional one [31]. The dynamics in the new phase space was formulated via an n -linear fully antisymmetric Nambu bracket with two or more “Hamiltonians”; as an example, Nambu applied his formalism to the free rigid body. ii) Hinted by an article by Deprit [32] and using the $SL(2, \mathbb{R})$ symmetry of the Euler equations,

in 1991 Holm and Marsden built a new Hamiltonian in such a way that the new dynamical system, so called in the literature *extended rigid body*, can be written as a Lie-Poisson system whose different Lie algebras structures can be $SO(3)$, $ISO(2)$ or $Heis_3$ [33]; particularly interesting is the $ISO(2)$ case, where the phase space of the Eulerian top is filled with invariant elliptic cylinders, on each of which, the dynamics, in elliptic coordinates, is the dynamics of a standard simple pendulum. iii) In 1995 R. Montgomery computed the change in the geometric phase for the attitude of the rigid body when the angular momentum vector in the body frame performs one period of its motion [34]. iv) Finally in 2017 [35] the free rotation of a classical rigid body was used in the control of two-level quantum systems by means of external electromagnetic pulses. In particular, authors showed that the dynamics of a rigid body can be used to implement one-qubit quantum gates.

In this paper we are interested in explore deeper the relation between the extended rigid body and the simple pendulum. As we have mentioned above, in the original paper [33] Holm and Marsden showed that the different Lie algebras structures of the extended rigid body are $SO(3)$, $ISO(2)$ or $Heis_3$, however in [36] authors showed that the complete list of possible Lie algebras are all the ones related to $SO(3)$ via analytical continuation and group contractions, which means that the algebra $ISO(1,1)$ must be also included. Even more, according to [33] the pendulum can be obtained from the extended rigid body if, from the geometrical point of view, the surfaces of the two new Casimir functions have the shape of elliptic cylinders, which leads to the fact that the corresponding Lie algebra is $ISO(2)$. Very recently using a representation of the rigid body in terms of two free parameters e_0 and κ [37] instead of the usual five parameters: energy E , magnitude of the angular momentum L , and the three principal moments of inertia I_1 , I_2 and I_3 , the classification of the inequivalent $SL(2, \mathbb{R})$ combinations of the Casimir functions was discussed both algebraically and geometrically. It turns out that whereas the geometry of the Casimir function that represents the square of the angular momentum continues being an S^2 sphere, the geometry of the Casimir function associated to the

kinetic energy which is an ellipsoid in the five parameters representation of the rigid body, is replaced by an elliptic hyperboloid that can be either of one or two sheets depending on the numerical values of both e_0 and κ , making the classification of the $SL(2, \mathbb{R})$ combinations of the Casimir functions richer. A result of this paper is to show that, considering all possible different geometries of the new Casimir functions, it is possible to obtain the pendulum also when the geometries associated to them are an elliptic cylinder and a hyperbolic cylinder. Specifically, when the cotangent space of the simple pendulum is given by the elliptic cylinder, the Lie algebra of the Hamiltonian vector fields associated to the coordinates in the rigid body-fixed frame is $ISO(2)$, whereas if the cotangent space is given by the hyperbolic cylinder, the Lie algebra is $ISO(1, 1)$. Even more, we show explicitly that for the $ISO(2)$ case we always obtain the whole set of motions of the pendulum whereas for the $ISO(1, 1)$ case we get the circulating motions but not the oscillatory ones. To the best of our knowledge this result has not been discussed previously in the literature.

Our exposition is as self-contained as possible. Section 2 is dedicated to summarize the main characteristics of the rigid body and its equations of motion, specially the $SL(2, \mathbb{R})$ symmetry of the later. In section 3 we discuss the Hamiltonian structure of the simple pendulum as function of both a real time and an imaginary time. The study of the whole $SL(2, \mathbb{R})$ transformations can be divided in three general sets where each set contains different fixed forms of the $SL(2, \mathbb{R})$ matrices. One of the three sets does not give origin to the pendulum and therefore we focus on the other two. Section 4 is devoted to the set of matrices where the relation between the rigid body and the simple pendulum can be established. This set can be subdivided in two general cases determined by the geometry of the Casimir functions, subsection 4.1 is dedicated to the case where both Casimir functions are given geometrically by elliptic cylinders whereas subsections 4.2 and 4.3 are dedicated to the study of the cases where one Casimir function has the geometry of an elliptic cylinder and the another Casimir function has the geometry of a hyperbolic cylinder. In section 5 we discuss the third and last set; as we will argue, this set is a limiting case of the

one in section 4 and therefore there does also exist a relation between the simple pendulum and the rigid body. Our conclusions are given in section 6.

2. The Euler equations and its $SL(2, \mathbb{R})$ symmetry

The torque free rigid body motion is one of the best understood systems in physics and the amount of papers and books discussing their dynamical properties is overwhelming. However there are still some properties related to this system that deserve to be explored further. In this section we give a short summary of the characteristics of the system that are relevant for our analysis of the relation between the so called *extended rigid body* and the *simple pendulum*. We base our discussion in [20, 33, 19, 37].

2.1. The Euler equations and the Casimir functions

It is well known that in a body-fixed reference frame the motion of the rigid body is governed by the Euler equations (see for instance [19])

$$\frac{d\vec{L}}{dt} = \vec{L} \times I^{-1} \vec{L}, \quad (1)$$

where \vec{L} is the vector of angular momentum and I is the moment of inertia tensor. If the body-fixed frame is oriented to coincide with the principal axes of inertia, the tensor I is diagonal. Without losing generality in the following discussion we consider that the principal moments of inertia satisfy the inequality

$$I_1 < I_2 < I_3. \quad (2)$$

When written in a basis, the L_i components of the angular momentum are the generators of a $SO(3)$ Lie algebra

$$[L_i, L_j] = \varepsilon_{ijk} L_k. \quad (3)$$

The system has two Casimir functions, the rotational kinetic energy C_1 and the square of the angular momentum C_2 , which are given in terms of the moments of inertia and the components of \vec{L} as

$$C_1(L_1, L_2, L_3) \equiv \frac{L_1^2}{2I_1} + \frac{L_2^2}{2I_2} + \frac{L_3^2}{2I_3}, \quad (4)$$

and

$$C_2(L_1, L_2, L_3) \equiv L_1^2 + L_2^2 + L_3^2, \quad (5)$$

respectively. The dynamical problem is usually solved using the Poinsot construction, in an Euclidean space \mathbb{R}^3 whose coordinates are the components of the angular momentum. When the vector \vec{L} moves relative to the axes of inertia of the top, it lies along the curve of intersection of the surfaces $C_1 = E = \text{constant}$ (an ellipsoid with semiaxes $\sqrt{2EI_1}$, $\sqrt{2EI_2}$ and $\sqrt{2EI_3}$) and $C_2 = L^2 = \text{constant}$ (a sphere of radius L). Because $2EI_1 < L^2 < 2EI_3$, the radius of the sphere has a value between the minimum and maximum values of the semiaxes of the ellipsoid. At first sight the solutions of the Euler equations (1) depend on five different parameters, the three moments of inertia, the energy E and the square of the angular momentum L^2 . However it has been shown that the problem can be rewritten in such a way that the solutions depend only on two parameters [22, 25, 20, 27]. The first parameter e_0 is related to the quotient E/L^2 whereas the second parameter κ codifies the values of the three moments of inertia, specifically, if \mathcal{I} is the diagonal matrix $\mathcal{I} = \text{diag}(1/I_1, 1/I_2, 1/I_3)$, then the relation between the five parameters: $\{I_i\}$, E and L^2 with the four parameters: $\{e_i\}$ and e_0 is given by

$$\frac{1}{I_i} - \frac{1}{3} \text{Tr } \mathcal{I} \equiv \sqrt{\frac{g_2}{3}} e_i \quad \frac{2E}{L^2} - \frac{1}{3} \text{Tr } \mathcal{I} \equiv \sqrt{\frac{g_2}{3}} e_0, \quad (6)$$

with $i = 1, 2, 3$ and

$$g_2 \equiv \frac{2}{3} \left[\left(\frac{1}{I_1} - \frac{1}{I_2} \right)^2 + \left(\frac{1}{I_2} - \frac{1}{I_3} \right)^2 + \left(\frac{1}{I_3} - \frac{1}{I_1} \right)^2 \right] > 0. \quad (7)$$

Notice that the new four parameters are dimensionless, and abusing of the language we can call to the set $\{e_i\}$ *dimensionless inertia parameters*, analogously although e_0 is not the energy of the system we can call it the *dimensionless energy parameter*. The dimensionless inertia parameters can be written in terms of only one angular parameter κ in the form

$$e_1 = \cos(\kappa), \quad e_2 = \cos(\kappa - 2\pi/3), \quad e_3 = \cos(\kappa + 2\pi/3), \quad (8)$$

and they are restricted to satisfy the conditions

$$e_1 + e_2 + e_3 = 0, \quad e_1^2 + e_2^2 + e_3^2 = 3/2 \quad \text{and} \quad e_1 e_2 e_3 = (\cos 3\kappa)/4. \quad (9)$$

Geometrically, in the three dimensional space $\{e_1, e_2, e_3\}$, the first condition in (9) represents a plane crossing the origin and the second condition represents a sphere of radius $\sqrt{3/2}$. The intersection of these two surfaces is a circle which is parameterized by the angular parameter κ . The role of g_2 (equation (7)) is to change the size of the sphere and therefore the size of the intersecting circle. It is clear that given a specific rigid body or equivalently a set of values for the three principal moments of inertia I_i , the value of the angular parameter κ is completely determined.

In general $\kappa \in [0, 2\pi]$, but notice that the condition (2) in terms of the dimensionless inertia parameters is obtained if the free parameter κ takes values in the subinterval $\kappa \in (0, \pi/3)$, i.e.

$$e_3 < e_2 < e_1. \quad (10)$$

The other five subintervals of length $\pi/3$ produce the other five possible orders for the e_i 's, for instance, if $\kappa \in (\pi/3, 2\pi/3)$ the parameters ordering is $e_3 < e_1 < e_2$, etc. For any value of κ , at least one of the inertia parameters is positive, another is negative and the third one may be either, positive, null or negative. Throughout all the paper we work in the interval $\kappa \in (0, \pi/3)$, for which $e_1 > 0$, $e_3 < 0$ and e_2 can be either positive, negative or null.

Finally introducing the dimensionless coordinates $u_i \equiv L_i/L$, the Euler equations (1) are rewritten as

$$\frac{du_i}{dt} = \frac{1}{2} \sqrt{\frac{g_2}{3}} L \varepsilon_{ijk} (e_k - e_j) u_j u_k. \quad (11)$$

It is possible to absorb the factor $\sqrt{\frac{g_2}{3}} L$, by defining a dimensionless time parameter: $x \equiv t \sqrt{\frac{g_2}{3}} L$, obtaining

$$\dot{u}_i = \frac{1}{2} \varepsilon_{ijk} (e_k - e_j) u_j u_k, \quad (12)$$

where (\cdot) denotes derivative with respect to the dimensionless time x . In a similar fashion Casimir functions (4) and (5) read now as

$$C_1(u_1, u_2, u_3) \equiv e_1 u_1^2 + e_2 u_2^2 + e_3 u_3^2, \quad (13)$$

$$C_2(u_1, u_2, u_3) \equiv u_1^2 + u_2^2 + u_3^2. \quad (14)$$

In the dimensionless angular momentum space \mathbb{R}^3 : (u_1, u_2, u_3) , $C_2 = 1$ and it represents a unitary sphere, whereas for the other Casimir: $C_1 = e_0$ and the ellipsoid (4), is replaced by an elliptic hyperboloid that can be either of one or two sheets depending on the numerical values of both $2E/L^2$ and κ , or equivalently on the number of positive and negative coefficients (dimensionless inertia parameters) in the equation. In this latter case the Casimir surface can also have the geometry of an elliptic cone or a hyperbolic cylinder in the proper limit situations. A complete classification of the geometrical shapes of the Casimir surface C_1 can be found in [37].

Regarding the solutions of the Euler equations (12), given the ordering (10) of the dimensionless inertia parameters, the solutions depend of the relative value between e_0 and e_2 . Here we are not going into details, but for purposes of completeness in our exposition, we present the explicit solutions, details can be found for instance in [20].

I. Case $e_3 < e_2 < e_0 < e_1$ (i.e. $1/I_2 < 2E/L^2$).

When the energy parameter e_0 is between the inertia parameters e_2 and e_1 , the solutions are given by

$$\begin{aligned} u_1(\tau) &= \text{sn}(\tau', m_c) \text{dn}(\tau, m), & u_2(\tau) &= \text{dn}(\tau', m_c) \text{sn}(\tau, m), \\ u_3(\tau) &= \text{cn}(\tau', m_c) \text{cn}(\tau, m), \end{aligned} \quad (15)$$

where τ is a dimensionless time parameter defined as

$$\tau = x \sqrt{(e_1 - e_2)(e_0 - e_3)}. \quad (16)$$

Here the amplitudes of the solutions are written as Jacobi elliptic functions at parameter $\tau' = \text{constant}$ and are related to the dimensionless parameters e_i and

e_0 in the form

$$\operatorname{sn}^2(\tau', m_c) = \frac{e_0 - e_3}{e_1 - e_3}, \quad \operatorname{cn}^2(\tau', m_c) = \frac{e_1 - e_0}{e_1 - e_3}, \quad \operatorname{dn}^2(\tau', m_c) = \frac{e_1 - e_0}{e_1 - e_2}. \quad (17)$$

The square modulus m and the complementary modulus m_c in the equation (15) are given by

$$\begin{aligned} m^2 &\equiv \frac{(e_2 - e_3)}{(e_0 - e_3)} \frac{(e_1 - e_0)}{(e_1 - e_2)} = \frac{(e_1 - e_0)}{(e_0 - e_3)} \frac{k_1^2}{k_2^2}, \quad \text{and} \\ m_c^2 &\equiv \frac{(e_0 - e_2)}{(e_0 - e_3)} \frac{(e_1 - e_3)}{(e_1 - e_2)} = \frac{(e_0 - e_2)}{(e_0 - e_3)} \frac{1}{k_2^2}, \end{aligned} \quad (18)$$

which take values in the interval $0 < m^2 < 1$ and $0 < m_c^2 < 1$ and satisfy $m^2 + m_c^2 = 1$. Here the quotients

$$k_1^2 = \frac{e_2 - e_3}{e_1 - e_3}, \quad \text{and} \quad k_2^2 = \frac{e_1 - e_2}{e_1 - e_3}, \quad (19)$$

satisfy in a similar way $k_1^2 + k_2^2 = 1$.

II. Case $e_3 < e_0 < e_2 < e_1$ (i.e. $2E/L^2 < 1/I_2$).

In this case the solutions are given by

$$\begin{aligned} u_1 &= \operatorname{cn}\left(\tau', i \frac{m_c}{m}\right) \operatorname{cn}\left(m\tau, \frac{1}{m}\right), \quad u_2 = \operatorname{dn}\left(\tau', i \frac{m_c}{m}\right) \operatorname{sn}\left(m\tau, \frac{1}{m}\right), \\ u_3 &= \operatorname{sn}\left(\tau', i \frac{m_c}{m}\right) \operatorname{dn}\left(m\tau, \frac{1}{m}\right), \end{aligned} \quad (20)$$

where the square modulus of the elliptic function take values in the interval $0 < 1/m^2 < 1$, with m^2 as defined in (18) but due to the fact that $e_3 < e_0 < e_2 < e_1$, $m^2 > 1$. The time parameter τ is the one defined in (16), whereas the amplitudes are written as Jacobi elliptic functions at parameter $\tau' = \text{constant}$

$$\begin{aligned} \operatorname{sn}^2\left(\tau', i \frac{m_c}{m}\right) &= \frac{e_1 - e_0}{e_1 - e_3}, \quad \operatorname{cn}^2\left(\tau', i \frac{m_c}{m}\right) = \frac{e_0 - e_3}{e_1 - e_3}, \\ \operatorname{dn}^2\left(\tau', i \frac{m_c}{m}\right) &= \frac{e_0 - e_3}{e_2 - e_3}. \end{aligned} \quad (21)$$

Physical interpretation of the solutions is straightforward, the curves (15) and (20) are the parameterization of the intersection of the unitary sphere of angular momentum and the corresponding surface of the Casimir function (13) [37] (see figure 1).

At this point it is convenient to make clear the possible values that can take the square modulus m^2 , the complementary modulus m_c^2 , their inverse values and the quotients of these quantities. The reason for it, is that these quantities will appear when the connection between the rigid body and the simple pendulum be established.

	m^2	m_c^2	$\frac{1}{m^2}$	$-\frac{m_c^2}{m^2}$	$\frac{1}{m_c^2}$	$-\frac{m^2}{m_c^2}$
$e_2 < e_0$	(0, 1)	(0, 1)	(1, ∞)	($-\infty$, 0)	(1, ∞)	($-\infty$, 0)
$e_0 < e_2$	(1, ∞)	($-\infty$, 0)	(0, 1)	(0, 1)	($-\infty$, 0)	(1, ∞)

Table 1: Intervals of values of the square modulus m^2 , complementary modulus m_c^2 , their inverse values $1/m^2$, $1/m_c^2$ and the quotients m^2/m_c^2 and m_c^2/m^2 , as functions of the relative values between the dimensionless energy parameter e_0 and the dimensionless inertia parameter e_2 .

Notice that, in an analogous way to the fact that m^2 and m_c^2 are complementary to each other in the sense that $m^2 + m_c^2 = 1$, the couple $1/m^2$ and $-m_c^2/m^2$ are complementary to each other, as well as the couple $1/m_c^2$ and $-m^2/m_c^2$, i.e.

$$m^2 + m_c^2 = 1, \quad \frac{1}{m^2} - \frac{m_c^2}{m^2} = 1, \quad \frac{1}{m_c^2} - \frac{m^2}{m_c^2} = 1. \quad (22)$$

2.2. $SL(2, \mathbb{R})$ symmetries of the Euler equations

In order to make manifest the gauge symmetries of the Euler equations, we notice that its dimensionless form

$$\dot{\vec{u}} = \vec{u} \times \epsilon \vec{u} \quad (23)$$

with ϵ a diagonal matrix of the form $\epsilon = \text{diag}(e_1, e_2, e_3)$, can be rewritten as the gradient of two scalar functions

$$\dot{\vec{u}} = \nabla l \times \nabla h, \quad (24)$$

where

$$h \equiv \frac{1}{2} C_1(u_1, u_2, u_3) - \frac{1}{2} e_0 = 0 \quad \Rightarrow \quad \epsilon \vec{u} = \nabla h = (e_1 u_1, e_2 u_2, e_3 u_3), \quad (25)$$

$$l \equiv \frac{1}{2} C_2(u_1, u_2, u_3) - \frac{1}{2} = 0 \quad \Rightarrow \quad \vec{u} = \nabla l = (u_1, u_2, u_3). \quad (26)$$

This form of writing the Euler equations makes explicit its invariance under any $SL(2, \mathbb{R})$ transformation [33]. It is straightforward to check that the transformation

$$\begin{pmatrix} \mathcal{H} \\ \mathcal{N} \end{pmatrix} = \begin{pmatrix} a & b \\ c & d \end{pmatrix} \begin{pmatrix} h \\ l \end{pmatrix}, \quad (27)$$

with $ad - bc = 1$ leads to

$$\dot{\vec{u}} = \nabla \mathcal{N} \times \nabla \mathcal{H}. \quad (28)$$

At this point we can consider either of the new Casimir surfaces \mathcal{N} or \mathcal{H} as the Hamiltonian surface. The systems that have this property are called bi-hamiltonian (see for instance [31, 19]). Usually the one that is chosen as the hamiltonian surface is \mathcal{H} , thus, given a dynamical system with Hamiltonian H , any dynamical quantity Q evolves with time according to

$$\dot{Q} = X_{\mathcal{H}} Q, \quad (29)$$

where the generator X_G is given by

$$X_G = (\nabla \mathcal{N} \times \nabla G) \cdot \nabla. \quad (30)$$

Notice that we are denoting with a different letter to the Hamiltonian or Casimir function: $H = H(u_1, u_2, u_3)$ and to the Casimir surface: $\mathcal{H}(u_1, u_2, u_3) \equiv H(u_1, u_2, u_3) - E = 0$.

According to the transformation (27), the generator X_G in components form is expressed as

$$\begin{aligned} X_G = & (ce_1 + d)u_1 \left(\frac{\partial G}{\partial u_2} \frac{\partial}{\partial u_3} - \frac{\partial G}{\partial u_3} \frac{\partial}{\partial u_2} \right) + (ce_2 + d)u_2 \left(\frac{\partial G}{\partial u_3} \frac{\partial}{\partial u_1} - \frac{\partial G}{\partial u_1} \frac{\partial}{\partial u_3} \right) \\ & + (ce_3 + d)u_3 \left(\frac{\partial G}{\partial u_1} \frac{\partial}{\partial u_2} - \frac{\partial G}{\partial u_2} \frac{\partial}{\partial u_1} \right). \end{aligned} \quad (31)$$

In order to determine the structure of the Lie algebra, we calculate the Lie-Poisson brackets for the Hamiltonian vector fields associated with the coordinate functions u_i

$$\begin{aligned} X_{u_1} &= (ce_3 + d)u_3 \partial_2 - (ce_2 + d)u_2 \partial_3, \\ X_{u_2} &= (ce_1 + d)u_1 \partial_3 - (ce_3 + d)u_3 \partial_1, \\ X_{u_3} &= (ce_2 + d)u_2 \partial_1 - (ce_1 + d)u_1 \partial_2. \end{aligned} \quad (32)$$

Explicitly, the Lie-Poisson brackets are given by

$$[X_{u_1}, X_{u_2}] = (ce_3 + d)X_{u_3}, \quad [X_{u_2}, X_{u_3}] = (ce_1 + d)X_{u_1}, \quad [X_{u_3}, X_{u_1}] = (ce_2 + d)X_{u_2}. \quad (33)$$

Regarding the classification of the different Lie algebras that arise from the $SL(2, \mathbb{R})$ invariant orbits, it turns out that, besides the $SO(3)$ Lie algebra (3) which corresponds to the rigid body, the algebras $SO(2, 1)$, $ISO(2)$, $ISO(1, 1)$ and $Heis_3$, also emerge. The systems corresponding to these algebras are termed under the name *extended rigid bodies*. The whole classification can be found, for instance, in [37].

Because is relevant for our discussion, it is important to emphasize that if instead we take the Casimir surface \mathcal{N} as the Hamiltonian surface, then the generator X_G is given by

$$X_G = -(\nabla \mathcal{H} \times \nabla G) \cdot \nabla \quad \Rightarrow \quad \dot{Q} = X_{\mathcal{N}} Q. \quad (34)$$

Clearly $X_{\mathcal{N}} = -X_{\mathcal{H}}$. If we denote as \tilde{X}_{u_i} to the Hamiltonian vector fields associated to the coordinates, we obtain in this case

$$\begin{aligned} \tilde{X}_{u_1} &= -(ae_3 + b)u_3\partial_2 + (ae_2 + b)u_2\partial_3, \\ \tilde{X}_{u_2} &= -(ae_1 + b)u_1\partial_3 + (ae_3 + b)u_3\partial_1, \\ \tilde{X}_{u_3} &= -(ae_2 + b)u_2\partial_1 + (ae_1 + b)u_1\partial_2. \end{aligned} \quad (35)$$

With these vector fields the Lie-Poisson brackets are given explicitly by

$$\begin{aligned} [\tilde{X}_{u_1}, \tilde{X}_{u_2}] &= -(ae_3 + b)\tilde{X}_{u_3}, & [\tilde{X}_{u_2}, \tilde{X}_{u_3}] &= -(ae_1 + b)\tilde{X}_{u_1}, \\ [\tilde{X}_{u_3}, \tilde{X}_{u_1}] &= -(ae_2 + b)\tilde{X}_{u_2}. \end{aligned} \quad (36)$$

The classification of the different Lie-Algebras coincide with the five mentioned above. Details are completely analogous to the previous ones and we do not discuss them further.

3. The pendulum

As in the case of the extended rigid body, solutions of the simple pendulum system are given in terms of Jacobi elliptic functions which are defined in the

whole complex plane \mathbb{C} and are doubly periodic. Due to the relevance of the expressions of the pendulum energy in both real and imaginary time, for the purposes of this paper, in this section we review briefly the main characteristics of the mathematical formulation of the simple pendulum. This is a well understood system and there are many interesting papers and books on the subject [4, 7, 9, 10, 11, 38, 39, 40]. In our discussion we follow [12] mainly.

3.1. Real time pendulum and solutions

Let us start considering a pendulum of point mass m and length r , in a constant downwards gravitational field, of magnitude $-g$ ($g > 0$). If θ is the polar angle measured counterclockwise respect to the vertical line and $\dot{\theta}$ stands for the time derivative of this angular position, the lagrangian of the system is given by

$$L(\theta, \dot{\theta}) = \frac{1}{2}mr^2\dot{\theta}^2 - mgr(1 - \cos \theta). \quad (37)$$

Here the zero of the potential energy is set at the lowest vertical position of the pendulum ($\theta = 2n\pi$, with $n \in \mathbb{Z}$). The equation of motion for this system is

$$\ddot{\theta} + \frac{g}{r} \sin \theta = 0, \quad (38)$$

which after integration gives origin to the conservation of total mechanical energy

$$E = \frac{1}{2}mr^2\dot{\theta}^2 + 2mgr \sin^2\left(\frac{\theta}{2}\right) = \text{constant}. \quad (39)$$

Physical solutions of equation (39) exist only if $E \geq 0$. We can rewrite the equation in dimensionless form, in terms of the dimensionless energy parameter: $k_E^2 \equiv \frac{E}{2mgr}$, and the dimensionless real time variable: $x \equiv \sqrt{\frac{g}{r}}t \in \mathbb{R}$, obtaining

$$\left(\frac{p}{2}\right)^2 + \sin^2\left(\frac{\theta}{2}\right) = k_E^2, \quad (40)$$

where p is the dimensionless angular velocity: $p(x) \equiv d\theta/dx$. By inspection of the potential we conclude that the pendulum has four different types of solutions depending of the value of the constant k_E^2 :

- *Static equilibrium* ($\dot{\theta} = 0$): The trivial behavior occurs when either $k_E^2 = 0$ or $k_E^2 = 1$. In the first case, necessarily $\dot{\theta} = 0$. For the case $k_E^2 = 1$ we consider also the situation where $\dot{\theta} = 0$. In both cases, the pendulum does not move, it is in static equilibrium. When $\theta = 2n\pi$ the equilibrium is stable and when $\theta = (2n + 1)\pi$ the equilibrium is unstable.

- *Oscillatory motions* ($0 < k_E^2 < 1$): In these cases the pendulum swings to and fro, respect to a point of stable equilibrium. The analytical solutions are given by

$$\theta(x) = 2 \arcsin[k_E \operatorname{sn}(x - x_0, k_E)], \quad (41)$$

$$p(x) = 2 k_E \operatorname{cn}(x - x_0, k_E), \quad (42)$$

where the square modulus k^2 of the elliptic functions is given directly by the energy parameter: $k^2 \equiv k_E^2$. Here x_0 is a second constant of integration and appears when equation (40) is integrated out. It means physically that we can choose the zero of time arbitrarily. The period of the movement is $4K$, or restoring the dimension of time, $4K\sqrt{g/r}$, with K the quarter period of the elliptic function $\operatorname{sn}(x - x_0, k_E)$.

- *Asymptotical motion* ($k_E^2 = 1$ and $\dot{\theta} \neq 0$): In this case the angle θ takes values in the open interval $(-\pi, \pi)$ and therefore, $\sin(\theta/2) \in (-1, 1)$. The particle just reach the highest point of the circle. The analytical solutions are given by

$$\theta(x) = \pm 2 \arcsin[\tanh(x - x_0)], \quad (43)$$

$$p(x) = \pm 2 \operatorname{sech}(x - x_0). \quad (44)$$

The sign \pm corresponds to the movement from $(\mp\pi \rightarrow \pm\pi)$. Notice that $\tanh(x - x_0)$, takes values in the open interval $(-1, 1)$ if: $x - x_0 \in (-\infty, \infty)$. For instance if $\theta \rightarrow \pi$, $x - x_0 \rightarrow \infty$ and $\tanh(x - x_0)$ goes asymptotically to 1. It is clear that this movement is not periodic. In the literature it is common to

take $x_0 = 0$.

• *Circulating motions* ($k_E^2 > 1$): In these cases the momentum of the particle is large enough to carry it over the highest point of the circle, so that it moves round and round the circle, always in the same direction. The solutions that describe these motions are of the form

$$\theta(x) = \pm 2 \operatorname{sgn} \left[\operatorname{cn} \left(k_E(x - x_0), \frac{1}{k_E} \right) \right] \arcsin \left[\operatorname{sn} \left(k_E(x - x_0), \frac{1}{k_E} \right) \right] \quad (45)$$

$$p(x) = \pm 2 k_E \operatorname{dn} \left(k_E(x - x_0), \frac{1}{k_E} \right), \quad (46)$$

where the global sign (+) is for the counterclockwise motion and the (−) sign for the motion in the clockwise direction. The symbol $\operatorname{sgn}(x)$ stands for the piecewise sign function which we define in the form

$$\operatorname{sgn} \left[\operatorname{cn} \left(k_E(x - x_0), \frac{1}{k_E} \right) \right] = \begin{cases} +1 & \text{if } (4n - 1)K \leq k_E(x - x_0) < (4n + 1)K, \\ -1 & \text{if } (4n + 1)K \leq k_E(x - x_0) < (4n + 3)K, \end{cases} \quad (47)$$

and its role is to shorten the period of the function $\operatorname{sn}(k_E(x - x_0), 1/k_E)$ by half. This fact is in agreement with the expression for $p(x)$ because the period of the elliptic function $\operatorname{dn}(k_E(x - x_0), 1/k_E)$ is $2K/k_E$ instead of $4K/k_E$, which is the period of the elliptic function $\operatorname{sn}(k_E(x - x_0), 1/k_E)$. The square modulus k^2 of the elliptic functions is equal to the inverse of the energy parameter $0 < k^2 = 1/k_E^2 < 1$.

These are all the possible motions of the simple pendulum. It is straightforward to check that the solutions satisfy the equation of conservation of energy (40) by using the following relations between the Jacobi functions (in these relations the modulus satisfies $0 < k^2 < 1$) and its analogous relation for hyperbolic functions (which are obtained in the limit case $k = 1$)

$$\operatorname{sn}^2(x, k) + \operatorname{cn}^2(x, k) = 1, \quad (48)$$

$$\tanh^2(x) + \operatorname{sech}^2(x) = 1, \quad (49)$$

$$k^2 \operatorname{sn}^2(x, k) + \operatorname{dn}^2(x, k) = 1. \quad (50)$$

3.2. Imaginary time pendulum

In the analysis above, time was considered a real variable, and therefore in the solutions of the simple pendulum only the real quarter period K appeared. But Jacobi elliptic functions are defined in \mathbb{C} and, for instance, the function $\text{sn}(z, k)$ of square modulus $0 < k^2 < 1$, besides the real primitive period $4K$, owns a pure imaginary primitive period $2iK_c$, where K and K_c are the so called quarter periods (see for instance [7]). In 1878 Paul Appell clarified the physical meaning of the imaginary time and the imaginary period in the oscillatory solutions of the pendulum [41, 9], by introducing an ingenious trick, he reversed the direction of the gravitational field: $g \rightarrow -g$, i.e. now the gravitational field is upwards. In order the Newton equations of motion remain invariant under this change in the force, we must replace the real time variable t by a purely imaginary one: $\tau \equiv \pm it$. Implementing these changes in the equation of motion (38) leads to the equation

$$\frac{d^2\theta}{d\tau^2} - \frac{g}{r} \sin \theta = 0. \quad (51)$$

Writing this equation in dimensionless form requires the introduction of the pure imaginary time variable $y \equiv \pm \tau \sqrt{g/r} = \pm ix$. Integrating once the resulting dimensionless equation of motion gives origin to the following equation

$$\frac{1}{4} \left(\frac{d\theta}{dy} \right)^2 - \sin^2 \left(\frac{\theta}{2} \right) = -k_E^2, \quad (52)$$

which looks like equation (40) but with an inverted potential. In order to solve this equation, we should flip the sign in the potential and rewrite the equation in such a way that it looks similar to equation (40). To achieve this aim we start by shifting the value of the potential energy one unit such that its minimum value be zero. Adding a unit of energy to both sides of the equation leads to

$$\left(\frac{\mathbb{P}}{2} \right)^2 + \cos^2 \left(\frac{\theta}{2} \right) = 1 - k_E^2. \quad (53)$$

Here \mathbb{P} is the momentum as function of imaginary time. The second step is to rewrite the potential energy in such a form it coincides with the potential energy

of (40) and, in this way, allowing us to compare solutions. We can accomplish this by a simple translation of the graph, for instance, by translating it an angle of $\pi/2$ to the right. Defining $\theta' = \theta - \pi$, we obtain

$$\left(\frac{\mathbb{P}}{2}\right)^2 + \sin^2\left(\frac{\theta'}{2}\right) = 1 - k_E^2. \quad (54)$$

It is clear that $0 < 1 - k_E^2 < 1$ for oscillatory motions and $1 - k_E^2 < 0$ for the circulating ones. It is not the purpose of this paper to review the whole set of solutions with imaginary time. The reader interested in the detailed construction can see [12] for instance.

4. The pendulum from the extended rigid body ($c \neq 0$ and $d \neq 0$)

In this section we review the relation between the rigid body and the simple pendulum as originally discussed by Holm and Marsden [33], and we extend it to pendulums of imaginary time. In every case we discuss the geometrical and the algebraic characteristics of the relations.

A lesson learned from [33] is that, in order to have the pendulum from the rigid body it is necessary that the $SL(2, \mathbb{R})$ transformation of the Casimir functions lead to new ones that geometrically represent two perpendicular elliptic cylinders. In our parameterization, the mathematical conditions for this to happen is that

$$ae_i + b = 0, \quad \text{and} \quad ce_j + d = 0, \quad \text{with} \quad i \neq j. \quad (55)$$

However, due to the fact that the inertia parameters are not necessarily positive, these conditions are not attached to elliptical cylinders only, but also to hyperbolic cylinders [37]. In order to have control over all different possibilities to get pendulums from the rigid body it is necessary to list all different $SL(2, \mathbb{R})$ transformations that fulfill conditions (55). The transformations are divided into three general sets, where each set contains different fixed forms of the $SL(2, \mathbb{R})$ matrices. The three sets are determined by the conditions: i) $c \neq 0$ and $d \neq 0$. ii) $c \neq 0$ and $d = 0$ and iii) $c = 0$ and $d \neq 0$ [42]. In the latter case

a generic $SL(2, \mathbb{R})$ group element has the form

$$g = \begin{pmatrix} a & b \\ 0 & 1/a \end{pmatrix}, \quad \text{with } b \in \mathbb{R}. \quad (56)$$

We conclude that the surface \mathcal{N} is a unitary sphere and therefore in this case it is not possible to degenerate the surface to a cylinder. As a consequence the pendulum can not arise from group elements of this kind and we must analyze only the cases i) and ii). Because the case discussed by Holm and Marsden belongs to the first set of conditions, we analyze it in this section and leave the set: $c \neq 0$ and $d = 0$ for section 5.

The first step in our analysis is to fully classify the different cases belonging to the set $c \neq 0$ and $d \neq 0$ in which the Casimir surfaces \mathcal{H} and \mathcal{N} as defined in equation (27) fulfill conditions (55). It is clear that there are 6 different forms to satisfy these conditions. However these are not all independent, in fact, the difference between conditions: $ae_i + b = 0$ and $ce_j + d = 0$, with respect to conditions: $ae_j + b = 0$ and $ce_i + d = 0$, is that they interchange the role of the Casimir functions H and N . Thus we can restrict ourselves to the analysis of the three cases (55) for $i < j$. Because solutions (15) and (20) depend on the relative value of the parameter e_0 respect to e_2 , the classification of geometries for both \mathcal{H} and \mathcal{N} in general also depends on this relative value [37]. This fact increases the number of cases to five. We show in table 2 the different possible geometries for the Casimir H and in table 3 the corresponding ones for the Casimir N . It is important to stress that in this classification we are using the fact that the space $\{u_1, u_2, u_3\}$ is \mathbb{R}^3 .

Situation	$ae_1 + b$	$ae_2 + b$	$ae_3 + b$	\mathcal{H} surface
1	$= 0$	< 0	< 0	elliptic cylinder around u_1
2	> 0	$= 0$	< 0	hyperbolic cylinder around u_2 with focus on u_1 ($e_2 < e_0$)
3	> 0	$= 0$	< 0	hyperbolic cylinder around u_2 with focus on u_3 ($e_0 < e_2$)
4	> 0	> 0	$= 0$	elliptic cylinder around u_3

Table 2: Classification of the four different geometries for the Casimir function H , in the asymmetric extended rigid body.

Situation	$ce_1 + d$	$ce_2 + d$	$ce_3 + d$	\mathcal{N} surface
5	$= 0$	< 0	< 0	elliptic cylinder around u_1
6	> 0	$= 0$	< 0	hyperbolic cylinder around u_2 with focus on u_1 ($e_2 < e_0$)
7	> 0	$= 0$	< 0	hyperbolic cylinder around u_2 with focus on u_3 ($e_0 < e_2$)
8	> 0	> 0	$= 0$	elliptic cylinder around u_3

Table 3: Classification of the four different geometries for the Casimir function N , in the asymmetric extended rigid body.

It is clear the five different possibilities we are referring to correspond to the intersections: 1-6, 1-7, 1-8, 2-8 y 3-8. The one discussed by Holm and Marsden corresponds to the case of the intersection of two elliptical cylinders 1-8, however we have four more possibilities which correspond to the intersection of an elliptical cylinder and a hyperbolic cylinder. For the best of our knowledge these four cases have not been discussed in the literature; one of the aims of this section is to give them an interpretation as pendulums. At this point it is convenient to stress the two main differences between our analysis and the original discussion in [33]. 1) The discussion of Holm and Marsden was given using the moments of inertia (2) as parameters whereas here we are using a different parameterization, the one in terms of the dimensionless inertia parameters $\{e_i\}$, which produce slight differences in the discussion. 2) Additionally to the original momentum map $\{u_i\} \rightarrow \{u_i(\theta, p)\}$ whose main characteristic is to have a real pendulum momentum p or equivalently a real angular coordinate θ and a real time t , in our discussion we will consider also momentum maps where the real pendulum momentum p is rewritten as $p = i\mathbb{P}$ with the new momentum: $\mathbb{P} = -ip$ purely imaginary. As discussed in subsection 3.2 this momentum is a consequence of introducing a purely imaginary time. When time is real the final dimensionless angular momentum space remains \mathbb{R}^3 whereas the associated pendulum phase space is $\mathbb{R} \times S^1$. When time is purely imaginary the final angular momentum space is $\mathbb{R}^2 \times i\mathbb{R}$ whereas the pendulum phase space is built with a real coordinate θ and a purely imaginary momentum \mathbb{P} . We start discussing the original case of Holm and Marsden (1-8).

4.1. Intersection of two elliptic cylinders

Choosing the a, b, c and d nonvanishing values of the group element $g \in SL(2, \mathbb{R})$ to satisfy

$$ae_1 + b = ce_3 + d = 0, \quad (57)$$

fix two of the three free parameters of g . Substituting b and d in the expressions (27) for the Casimir surfaces we obtain

$$\mathcal{H} : -\frac{a}{2}(e_1 - e_2)u_2^2 - \frac{a}{2}(e_1 - e_3)u_3^2 = -\frac{a}{2}(e_1 - e_0), \quad (58)$$

$$\mathcal{N} : \frac{c}{2}(e_1 - e_3)u_1^2 + \frac{c}{2}(e_2 - e_3)u_2^2 = \frac{c}{2}(e_0 - e_3). \quad (59)$$

Notice that the surfaces do not depend of the specific values of both a and c . However we can fix one of these parameters in terms of the other using the condition $ad - bc = 1$, which in this case produce the condition $ac = 1/(e_1 - e_3)$. In other words, Holm and Marsden considered an element $g \in SL(2, \mathbb{R})$ of the type

$$g = \begin{pmatrix} \frac{1}{c(e_1 - e_3)} & -\frac{e_1}{c(e_1 - e_3)} \\ c & -ce_3 \end{pmatrix}, \quad (60)$$

which depends only on one free parameter $c \neq 0$. Originally this parameter was fixed to the value $c = 1$ although it is not necessary to fix it because the $SL(2, \mathbb{R})$ combination of h and l leads to expressions that do not depend on c . It is clear that given the ordering (10), the coefficients in (60) have the property $a > 0, b < 0$ and $d > 0$.

The equations that determine the Casimir surfaces can be written finally as

$$\mathcal{H} : k_2^2 u_2^2 + u_3^2 = \frac{e_1 - e_0}{e_1 - e_3}, \quad (61)$$

$$\mathcal{N} : u_1^2 + k_1^2 u_2^2 = \frac{e_0 - e_3}{e_1 - e_3}, \quad (62)$$

which generically represent two elliptic cylinders, \mathcal{H} with axis on coordinate u_1 and \mathcal{N} with axis along u_3 . Here k_1^2 and k_2^2 are the ones defined in (19). At this point the transverse sections of the cylinders are ellipses whose semi-major and semi-minor axes depend on the value of the parameter e_0 , i.e. they have variable size and the intersections are exactly the same as the ones in fig. 1(a)

because the $SL(2, \mathbb{R})$ transformations change the geometry of the Casimirs but leave invariant the intersections [31].

The strategy is now to implement a variable change in such a way that one of the cylinders becomes circular using only trigonometric functions. Once this aim is achieved, the second cylinder can not be mapped to a circular cylinder simultaneously without introducing elliptic functions. This strategy can be applied in two different ways, in one case \mathcal{H} becomes the circular cylinder, whereas in the second case the Casimir whose geometry becomes the circular cylinder is \mathcal{N} . Interestingly these two cases produce the same physical system as expected for a bi-hamiltonian system, although the physical origin differs in both cases as we will explain. The variable changes or technically the momentum maps we implement [19], are analogous to the one performed by Holm and Marsden. As a result of the mapping one of the resulting Casimir functions obtain the form of the Hamiltonian of the simple pendulum and we can identify directly if the energy produces an oscillating or a circulating movement. Additionally we also introduce momentum maps for imaginary time.

- Simple pendulum with real time and Hamiltonian \mathcal{H} : Consider the momentum map

$$u_1 \equiv \sqrt{\frac{e_0 - e_3}{e_1 - e_3}} \cos\left(\frac{\theta}{2}\right), \quad u_2 \equiv \frac{1}{k_1} \sqrt{\frac{e_0 - e_3}{e_1 - e_3}} \sin\left(\frac{\theta}{2}\right), \quad u_3 \equiv \frac{k_2}{k_1} \sqrt{\frac{e_0 - e_3}{e_1 - e_3}} \frac{p}{2}. \quad (63)$$

The expression for the Casimir surface \mathcal{N} is explicitly satisfied whereas the expression for the Casimir \mathcal{H} becomes

$$\mathcal{H} : \sin^2\left(\frac{\theta}{2}\right) + \left(\frac{p}{2}\right)^2 = \frac{e_1 - e_0}{e_0 - e_3} \cdot \frac{e_2 - e_3}{e_1 - e_2} \equiv m^2. \quad (64)$$

\mathcal{N} is interpreted as the cotangent space and has the geometry of a circular cylinder of unitary radius. On the other side, according to equation (40) \mathcal{H} is the Hamiltonian of a pendulum. This is the analogous of the relation found by Holm and Marsden [33]. Because situation 1 in table 2 is valid for any value of e_0 in the interval $e_3 < e_0 < e_1$ we have that $0 < m^2 < 1$ for $e_0 > e_2$, $m^2 = 1$ for

$e_0 = e_2$ and $m^2 > 1$ for $e_0 < e_2$ (see table 1). Therefore for $m^2 < 1$ we have an oscillatory movement of the pendulum, for $m^2 = 1$ we have a critical movement and for $m^2 > 1$ we have a circulating one. Fig. 1(b) shows the complete phase space of the pendulum.

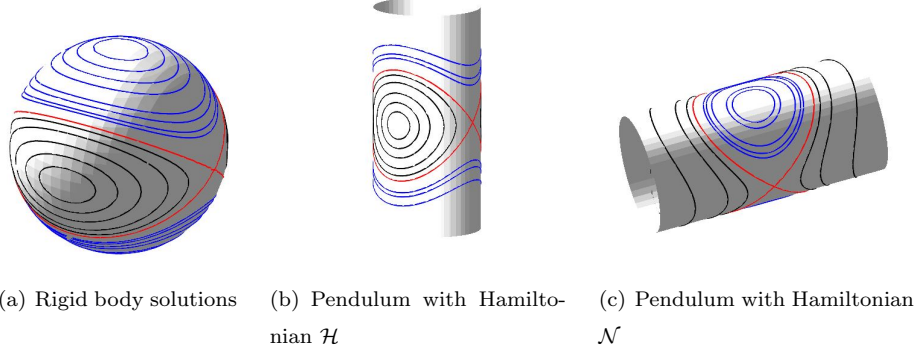


Figure 1: Figure 1(a) shows the solution trajectories of the vector of angular momentum in the body-fixed frame, for the $SO(3)$ rigid body. The ones corresponding to $e_2 < e_0$ are drawn in black whereas the ones corresponding to $e_0 < e_2$ are drawn in blue. The red lines correspond to the separatrices. Fig. 1(b) corresponds to the phase space of a simple pendulum with Hamiltonian \mathcal{H} and cotangent space \mathcal{N} . The oscillatory movements are drawn in black whereas the circulating ones are drawn in blue. The colors correspond to the ones in fig. 1(a) and represent the relation between them. Fig. 1(c) corresponds to the phase space of a simple pendulum with Hamiltonian \mathcal{N} and cotangent space \mathcal{H} . The oscillatory trajectories are drawn in blue whereas the circulating ones are drawn in black. The colors correspond to the ones in fig. 1(a) and represent the relation between them.

Regarding the generators (32) of the system, it is straightforward to check they can be redefined as

$$\begin{aligned}
 Y_{u_1} &\equiv \frac{1}{c\alpha} X_{u_1} = -\frac{(e_1 - e_3)}{\alpha} k_1^2 u_2 \partial_3, \\
 Y_{u_2} &\equiv \frac{k_1}{c\alpha} X_{u_2} = \frac{(e_1 - e_3)}{\alpha} k_1 u_1 \partial_3, \\
 Y_{u_3} &\equiv \frac{1}{ck_1(e_1 - e_3)} X_{u_3} = k_1 u_2 \partial_1 - \frac{1}{k_1} u_1 \partial_2,
 \end{aligned} \tag{65}$$

which satisfy the Lie-Poisson algebra $ISO(2)$

$$[Y_{u_1}, Y_{u_2}] = 0, \quad [Y_{u_2}, Y_{u_3}] = Y_{u_1}, \quad [Y_{u_3}, Y_{u_1}] = Y_{u_2}. \tag{66}$$

A Lie-Poisson structure for the pendulum can be introduced on the cylindrical surface $\mathcal{N} = 1$ [33], in terms of the variables θ, p by defining the Lie-Poisson bracket as

$$\{f, g\}_{\mathcal{N}} = -\nabla \mathcal{N} \cdot (\nabla f \times \nabla g). \quad (67)$$

An straightforward calculation gives

$$\{f, g\}_{\mathcal{N}} = -8 \frac{(e_1 - e_3)(e_2 - e_3)}{\sqrt{(e_1 - e_2)(e_0 - e_3)}} \left(\frac{\partial f}{\partial \theta} \frac{\partial g}{\partial p} - \frac{\partial f}{\partial p} \frac{\partial g}{\partial \theta} \right), \quad (68)$$

which shows that the variables θ and p are canonically conjugate up to a scale factor: $\{p, \theta\}_{\mathcal{N}} = 8 \frac{(e_1 - e_3)(e_2 - e_3)}{\sqrt{(e_1 - e_2)(e_0 - e_3)}}$. In terms of this bracket the canonical equations of motion are given by

$$\frac{d\theta}{d\tau} = \{\mathcal{H}, \theta\}_{\mathcal{N}} \quad \text{and} \quad \frac{dp}{d\tau} = \{\mathcal{H}, p\}_{\mathcal{N}}. \quad (69)$$

Combining these we obtain the Newton equation of motion for the simple pendulum

$$\frac{d^2\theta}{d\tau^2} = -16 \frac{(e_1 - e_3)^2 (e_2 - e_3)^2}{(e_1 - e_2)(e_0 - e_3)} \sin \theta. \quad (70)$$

- Simple pendulum with imaginary time and Hamiltonian \mathcal{H} : Consider the momentum map

$$u_1 \equiv \sqrt{\frac{e_0 - e_3}{e_1 - e_3}} \sin \left(\frac{\theta'}{2} \right), \quad u_2 \equiv \frac{1}{k_1} \sqrt{\frac{e_0 - e_3}{e_1 - e_3}} \cos \left(\frac{\theta'}{2} \right), \quad u_3 \equiv i \frac{k_2}{k_1} \sqrt{\frac{e_0 - e_3}{e_1 - e_3}} \frac{\mathbb{P}}{2}. \quad (71)$$

The expression for the Casimir surface \mathcal{N} is again explicitly satisfied whereas the form of the Casimir \mathcal{H} becomes

$$\mathcal{H} : \sin^2 \left(\frac{\theta'}{2} \right) + \left(\frac{\mathbb{P}}{2} \right)^2 = m_c^2, \quad (72)$$

where m_c^2 is the complementary modulus as defined in (18). The Casimir \mathcal{H} represents the Hamiltonian of the simple pendulum with imaginary time (54). Again because (72) is valid for any value of e_0 , we have all different movements of the pendulum. In particular for the oscillatory motions: $e_2 < e_0$ and $0 < m_c^2 < 1$, for the asymptotical motion: $e_0 = e_2$ and $m_c^2 = 0$, whereas for the

circulating movements: $e_0 < e_2$ and $m_c^2 < 0$ (see table 1). Notice that the explicit presence of the imaginary number i in coordinate u_3 geometrically plays the role of changing the elliptic cylinder into a hyperbolic cylinder although the former is defined in a real space \mathbb{R}^3 whereas the later is defined in a complex space $\mathbb{R}^2 \times i\mathbb{R}$. Regarding the Lie-Poisson algebra it is clear that here we have the same $ISO(2)$ algebra (66). The two dimensional Lie-Poisson bracket in this case has a purely imaginary scale factor

$$\{f, g\}_{\mathcal{N}} = -8i \frac{(e_1 - e_3)(e_2 - e_3)}{\sqrt{(e_1 - e_2)(e_0 - e_3)}} \left(\frac{\partial f}{\partial \theta} \frac{\partial g}{\partial \mathbb{P}} - \frac{\partial f}{\partial \mathbb{P}} \frac{\partial g}{\partial \theta} \right), \quad (73)$$

which is in agreement with the fact that the Newton equation for the simple pendulum with imaginary time has an extra minus sign in the force term

$$\frac{d^2\theta}{d\tau^2} = 16 \frac{(e_1 - e_3)^2(e_2 - e_3)^2}{(e_1 - e_2)(e_0 - e_3)} \sin \theta. \quad (74)$$

Because the rigid body is a bi-Hamiltonian system it is interesting to obtain the simple pendulum but now having the Casimir function \mathcal{N} as the hamiltonian and the Casimir function \mathcal{H} as the cotangent space.

- Simple pendulum with real time and Hamiltonian \mathcal{N} : Consider the momentum map

$$u_1 \equiv \frac{k_1}{k_2} \sqrt{\frac{e_1 - e_0}{e_1 - e_3}} \frac{p}{2}, \quad u_2 \equiv \frac{1}{k_2} \sqrt{\frac{e_1 - e_0}{e_1 - e_3}} \sin \left(\frac{\theta}{2} \right), \quad u_3 \equiv \sqrt{\frac{e_1 - e_0}{e_1 - e_3}} \cos \left(\frac{\theta}{2} \right). \quad (75)$$

Now the expression for the Casimir function \mathcal{H} is explicitly satisfied whereas the expression for the Casimir \mathcal{N} becomes

$$\mathcal{N} : \left(\frac{p}{2} \right)^2 + \sin^2 \left(\frac{\theta}{2} \right) = \frac{1}{m^2}, \quad (76)$$

which according to equation (40) corresponds to the energy of a simple pendulum. Because situation 8 in table 3 is valid for any value of e_0 in the interval $e_3 < e_0 < e_1$, in equation (76) we have all different movements of the pendulum. It is worth to stress that whereas for values $e_0 < e_2$ for which $0 < m^2 < 1$ the movements in (64) are oscillatory (see fig. 1(b)), in (76) for the same values

of e_0 : $1 < 1/m^2 < \infty$ and therefore we have circulating pendulums (see fig. 1(c)). Something analogous occur for the circulating movements in (64) and the oscillatory ones in (76). The asymptotical cases are given for $e_0 = e_2$ for which $m^2 = 1$ in both (64) and (76).

Let us emphasize that the circular cylinder \mathcal{H} has unitary radius. In this case the Hamiltonian vector field associated with the coordinates u_i 's are given by equations (35). Redefining these vector fields as

$$\begin{aligned}\tilde{Y}_{u_1} &\equiv \frac{1}{a(e_1 - e_3)k_2} \tilde{X}_{u_1} = \frac{1}{k_2} u_3 \partial_2 - k_2 u_2 \partial_3, \\ \tilde{Y}_{u_2} &\equiv \frac{1}{a\alpha} \tilde{X}_{u_2} = -\frac{(e_1 - e_3)}{\alpha} u_3 \partial_1, \\ \tilde{Y}_{u_3} &\equiv \frac{1}{a\alpha k_2} \tilde{X}_{u_3} = \frac{e_1 - e_3}{\alpha} k_2 u_2 \partial_1,\end{aligned}\tag{77}$$

they satisfy the $ISO(2)$ Lie-Poisson algebra

$$[\tilde{Y}_{u_1}, \tilde{Y}_{u_2}] = \tilde{Y}_{u_3}, \quad [\tilde{Y}_{u_2}, \tilde{Y}_{u_3}] = 0, \quad [\tilde{Y}_{u_3}, \tilde{Y}_{u_1}] = \tilde{Y}_{u_2}.\tag{78}$$

Regarding the Lie-Poisson bracket in terms of the variables (θ, p) on the cylindrical surface $\mathcal{H} = 1$, and defined as

$$\{f, g\}_{\mathcal{H}} = -\nabla \mathcal{H} \cdot (\nabla f \times \nabla g),\tag{79}$$

we have

$$\{f, g\}_{\mathcal{H}} = 8 \frac{(e_1 - e_3)(e_1 - e_2)}{\sqrt{(e_1 - e_0)(e_2 - e_3)}} \left(\frac{\partial f}{\partial \theta} \frac{\partial g}{\partial p} - \frac{\partial f}{\partial p} \frac{\partial g}{\partial \theta} \right).\tag{80}$$

The Newton equation associated to this Lie-Poisson bracket is

$$\frac{d^2\theta}{d\tau^2} = -16 \frac{(e_1 - e_3)^2 (e_1 - e_2)^2}{(e_1 - e_0)(e_2 - e_3)} \sin \theta.\tag{81}$$

- Simple pendulum with imaginary time and Hamiltonian \mathcal{N} : Consider the momentum map

$$u_1 \equiv i \frac{k_1}{k_2} \sqrt{\frac{e_1 - e_0}{e_1 - e_3}} \frac{\mathbb{P}}{2}, \quad u_2 \equiv \frac{1}{k_2} \sqrt{\frac{e_1 - e_0}{e_1 - e_3}} \cos \left(\frac{\theta'}{2} \right), \quad u_3 \equiv \sqrt{\frac{e_1 - e_0}{e_1 - e_3}} \sin \left(\frac{\theta'}{2} \right).\tag{82}$$

The expression for the Casimir function \mathcal{H} is explicitly satisfied whereas the expression for the Casimir \mathcal{N} becomes

$$\mathcal{N} : \left(\frac{\mathbb{P}}{2} \right)^2 + \sin^2 \left(\frac{\theta'}{2} \right) = -\frac{m_c^2}{m^2}. \quad (83)$$

This is the Hamiltonian of a simple pendulum with imaginary time. As in the previous cases, because (83) is valid for any value of e_0 , it includes all different movements of the pendulum. Because the cotangent space is \mathcal{H} , the $ISO(2)$ Lie-Poisson algebra is given by (78), and the Lie-Poisson bracket in terms of the variables (θ, \mathbb{P}) is similar to (80) and differs only by a factor of i in the scale factor.

The geometrical interpretation of these results is straightforward. If we start with a specific $SO(3)$ rigid body, the three moments of inertia $\{I_i\}$ are given, which fix the parameter κ and therefore the three dimensionless parameters of inertia $\{e_i\}$. The different solutions are obtained for different values of e_0 . After the $SL(2, \mathbb{R})$ gauge transformation of the Casimir surfaces, for the momentum maps (63) and (71) we obtain a unitary circular cylinder \mathcal{N} with the axis along the u_3 direction representing the cotangent space. On the other side, geometrically \mathcal{H} is an element of a set of elliptic-(hyperbolic) cylinders with axis along the u_1 direction which physically are energy surfaces, because \mathcal{H} is the Hamiltonian of the simple pendulum (see equations (40) and (54)). Intersections of the single circular cylinder \mathcal{N} with the set of elliptic-(hyperbolic) cylinders \mathcal{H} represent all the movements of the pendulum. On the other side, for the momentum maps (75) and (82) the surface \mathcal{H} becomes an unitary circular cylinder with axis along the u_1 direction representing the cotangent space and \mathcal{N} is an element of a set of elliptic-(hyperbolic) cylinders that represent the Hamiltonian of the simple pendulum.

4.2. Intersection of a hyperbolic cylinder and an elliptic cylinder I

Let us consider the cases 2-8 and 3-8, which correspond to the intersection of a hyperbolic cylinder and an elliptical cylinder. In these cases the $SL(2, \mathbb{R})$

group element has the form

$$g = \begin{pmatrix} \frac{1}{c(e_2-e_3)} & -\frac{e_2}{c(e_2-e_3)} \\ c & -ce_2 \end{pmatrix}. \quad (84)$$

As a consequence the Casimir surfaces are given by the expressions

$$\mathcal{H} : \quad k_2^2 u_1^2 - k_1^2 u_3^2 = \frac{e_0 - e_2}{e_1 - e_3}, \quad (85)$$

$$\mathcal{N} : \quad u_1^2 + k_1^2 u_2^2 = \frac{e_0 - e_3}{e_1 - e_3}. \quad (86)$$

Notice that the Casimir \mathcal{N} is exactly the same as (62), as it should be since in both cases we are dealing with the situation 8 (see table 3), which represents an elliptic cylinder of unitary radius with axis along u_3 . The cases 2-8 and 3-8 differ in the sign of the right hand side of the Casimir \mathcal{H} (85), for the case 2-8 we have $e_0 - e_2 > 0$, whereas for the case 3-8 we have $e_0 - e_2 < 0$. Geometrically the different signs change the orientation of the hyperbolic cylinders (see fig 2). Again we expect to have two different momentum maps, one in which \mathcal{N} is the cotangent space and \mathcal{H} is the Hamiltonian and a second one where \mathcal{H} is the cotangent space and \mathcal{N} is the Hamiltonian.

- Simple pendulum with real time and Hamiltonian \mathcal{H} : As we have discussed previously, under the momentum map (63)

$$u_1 \equiv \sqrt{\frac{e_0 - e_3}{e_1 - e_3}} \cos\left(\frac{\theta}{2}\right), \quad u_2 \equiv \frac{1}{k_1} \sqrt{\frac{e_0 - e_3}{e_1 - e_3}} \sin\left(\frac{\theta}{2}\right), \quad u_3 \equiv \frac{k_2}{k_1} \sqrt{\frac{e_0 - e_3}{e_1 - e_3}} \left(\frac{p}{2}\right),$$

the expression for the Casimir \mathcal{N} is automatically satisfied. On the other side the Casimir surface (85) coincides with the Hamiltonian (40) and (64)

$$\mathcal{H} : \sin^2\left(\frac{\theta}{2}\right) + \left(\frac{p}{2}\right)^2 = m^2,$$

where $0 < m^2 < 1$ for the case 2-8 ($e_0 - e_2 > 0$) and therefore represent the oscillatory movements, whereas $1 < m^2 < \infty$ for the case 3-8 ($e_0 - e_2 < 0$) which represent the circulating movements. As usual the case $e_0 = e_2$ produce the separatrix. Regarding the Hamiltonian vector fields associated to the co-ordinates, they are the same as (65) and therefore they satisfy the Lie-Poisson

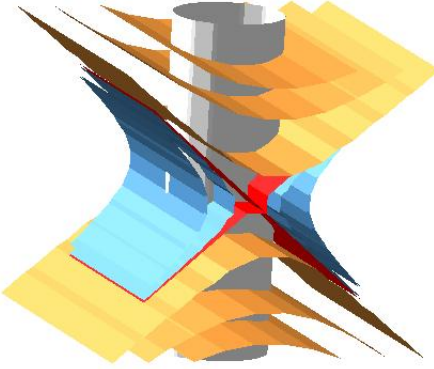


Figure 2: Figure shows the geometry of the hyperbolic cylinders for different values for e_0 . The geometry corresponding to $e_2 < e_0$ is drawn in blue whereas the ones corresponding to $e_0 < e_2$ are drawn in yellow. The red planes correspond to the separatrixes.

algebra $ISO(2)$ (66). A straightforward calculation gives the two dimensional Lie-Poisson bracket (68) and the Newton equation (70). These results show that this case and IV-A represent the same dynamics, although they come from a different geometry for the Casimir \mathcal{H} .

- Simple pendulum with imaginary time and Hamiltonian \mathcal{H} : As in section 4.1, under the momentum map

$$u_1 \equiv \sqrt{\frac{e_0 - e_3}{e_1 - e_3}} \sin\left(\frac{\theta'}{2}\right), \quad u_2 \equiv \frac{1}{k_1} \sqrt{\frac{e_0 - e_3}{e_1 - e_3}} \cos\left(\frac{\theta'}{2}\right), \quad u_3 \equiv i \frac{k_2}{k_1} \sqrt{\frac{e_0 - e_3}{e_1 - e_3}} \left(\frac{\mathbb{P}}{2}\right), \quad (87)$$

the expression for the Casimir \mathcal{N} is automatically satisfied whereas the Casimir \mathcal{H} becomes

$$\mathcal{H} : \sin^2\left(\frac{\theta'}{2}\right) + \left(\frac{\mathbb{P}}{2}\right)^2 = m_c^2. \quad (88)$$

where $-\infty < m_c^2 < 1$. Notice that the geometrical role of writing the coordinate

u_3 in terms of an imaginary momentum \mathbb{P} is to map the hyperbolic cylinder \mathcal{H} to an elliptic cylinder with axis along the u_2 direction. According to equation (54), \mathcal{H} represents the Hamiltonian for a simple pendulum of imaginary time and energy $m^2 = 1 - m_c^2$, as the one in (4.2). As expected, the two dimensional Lie-Poisson structure and Newton equations coincide with (73) and (74).

Next natural mapping is the one that maps the rigid body system to a cotangent space \mathcal{H} , with hamiltonian \mathcal{N} . By inspection of the Casimir (85), this can be achieved introducing a purely imaginary coordinate. Doing this allows to change the hyperbolic nature of the cylinders defined in \mathbb{R}^3 to elliptic cylinders defined in $\mathbb{R}^2 \times i\mathbb{R}$.

- Circulating simple pendulum with real time, imaginary coordinate and Hamiltonian \mathcal{N} : Consider the momentum map

$$u_1 \equiv \frac{1}{k_2} \sqrt{\frac{e_0 - e_2}{e_1 - e_3}} \sin\left(\frac{\theta}{2}\right), \quad u_2 \equiv \frac{1}{k_1 k_2} \sqrt{\frac{e_0 - e_2}{e_1 - e_3}} \frac{p}{2}, \quad u_3 \equiv \frac{i}{k_1} \sqrt{\frac{e_0 - e_2}{e_1 - e_3}} \cos\left(\frac{\theta}{2}\right). \quad (89)$$

Here we are assuming: $e_0 - e_2 > 0$ (situation 2 in table 2). For such a map the Casimir \mathcal{H} is automatically satisfied whereas the Casimir \mathcal{N} takes the form

$$\mathcal{N} : \sin^2\left(\frac{\theta}{2}\right) + \left(\frac{p}{2}\right)^2 = \frac{1}{m_c^2}, \quad (90)$$

where $1 < 1/m_c^2 < \infty$ (see table 1) and therefore the Hamiltonian equation represents only circulating movements of the simple pendulum.

Because the Hamiltonian is given by \mathcal{N} , the suitable Hamiltonian vector fields associated to the coordinates are given by equation (35). Redefining them as

$$\begin{aligned} \tilde{Y}_{u_1} &\equiv \frac{k_2}{a\beta k_1} \tilde{X}_{u_1} = \frac{1}{\beta} \sqrt{(e_1 - e_2)(e_2 - e_3)} u_3 \partial_2, \\ \tilde{Y}_{u_2} &\equiv \frac{1}{a\sqrt{(e_1 - e_3)(e_2 - e_3)}} \tilde{X}_{u_2} = -\frac{k_2}{k_1} u_1 \partial_2 - \frac{k_1}{k_2} u_3 \partial_1, \\ \tilde{Y}_{u_3} &\equiv \frac{1}{a\beta} \tilde{X}_{u_3} = \frac{1}{\beta} (e_1 - e_2) u_1 \partial_2, \end{aligned} \quad (91)$$

they satisfy the $ISO(1, 1)$ Lie-Poisson algebra

$$[\tilde{Y}_{u_1}, \tilde{Y}_{u_2}] = \tilde{Y}_{u_3}, \quad [\tilde{Y}_{u_2}, \tilde{Y}_{u_3}] = -\tilde{Y}_{u_1}, \quad [\tilde{Y}_{u_3}, \tilde{Y}_{u_1}] = 0. \quad (92)$$

Regarding the two-dimensional Lie-Poisson bracket, it has the form

$$\{f, g\}_{\mathcal{N}} = -8i \frac{(e_1 - e_2)(e_2 - e_3)}{\sqrt{(e_0 - e_2)(e_1 - e_3)}} \left(\frac{\partial f}{\partial \theta} \frac{\partial g}{\partial p} - \frac{\partial f}{\partial p} \frac{\partial g}{\partial \theta} \right), \quad (93)$$

while the equation of motion goes as:

$$\frac{d^2 \theta}{d\tau^2} = 16 \frac{(e_2 - e_3)^2 (e_1 - e_2)^2}{(e_1 - e_3)(e_0 - e_2)} \sin \theta, \quad (94)$$

At this point the sign in the Newton equation seems to be wrong, but this sign is reflecting the fact that we have applied a complex map in coordinate u_3 .

Although we have presented the analysis assuming $e_2 - e_0 < 0$, it is worth to point out that the same physical situation emerge also for the case $e_2 - e_0 > 0$. The only difference is to introduce a mapping where the complex coordinate is u_1 instead of u_3 . We get as a conclusion of this subsection that, for the situation where the intersection of Casimir functions is among a hyperbolic cylinder \mathcal{H} and a elliptic cylinder \mathcal{N} , if the Hamiltonian is given by \mathcal{H} and the cotangent space is given by \mathcal{N} then we get the whole motions of the simple pendulum and the Lie algebra of the extended rigid body is $ISO(2)$, but in the case where \mathcal{H} is the Hamiltonian and \mathcal{H} is the cotangent space we only get the circulating motions and the Lie algebra is $ISO(1, 1)$.

- Circulating simple pendulum with imaginary time, imaginary coordinate and Hamiltonian \mathcal{N} : Consider the mapping

$$u_1 \equiv \frac{1}{k_2} \sqrt{\frac{e_0 - e_2}{e_1 - e_3}} \cos \left(\frac{\theta'}{2} \right), \quad u_2 \equiv \frac{i}{k_1 k_2} \sqrt{\frac{e_0 - e_2}{e_1 - e_3}} \frac{\mathbb{P}}{2}, \quad u_3 \equiv \frac{i}{k_1} \sqrt{\frac{e_0 - e_2}{e_1 - e_3}} \sin \left(\frac{\theta'}{2} \right). \quad (95)$$

For such a map, where we are assuming $e_0 - e_2 > 0$, the Casimir \mathcal{H} is automatically satisfied whereas the Casimir \mathcal{N} takes the form

$$\mathcal{N} : \left(\frac{\mathbb{P}}{2} \right)^2 + \sin^2 \left(\frac{\theta'}{2} \right) = -\frac{m^2}{m_c^2}. \quad (96)$$

It is straightforward to notice that $-m^2/m_c^2 < 0$, and therefore we have as expected only circulating movements. This case also comes from the extend rigid body with Lie algebra $SO(1, 1)$. Regarding the two dimensional Lie-Poisson bracket it has the following expression

$$\{f, g\}_{\mathcal{N}} = 8 \frac{(e_1 - e_2)(e_2 - e_3)}{\sqrt{(e_0 - e_2)(e_1 - e_3)}} \left(\frac{\partial f}{\partial \theta} \frac{\partial g}{\partial \mathbb{P}} - \frac{\partial f}{\partial \mathbb{P}} \frac{\partial g}{\partial \theta} \right), \quad (97)$$

while the Newton equation of motion goes as (94) but with an extra minus sign in the right hand side of the equation. Again the discordance of the Newton equation with respect to equation (54) is understood by the fact that the momentum map (95) considers a complex transformation in coordinate u_3 .

4.3. Intersection of a hyperbolic cylinder and an elliptic cylinder II

As final cases we study the intersections between the elliptic cylinder and hyperbolic cylinder 1-6 and 1-7, for which the $SL(2, \mathbb{R})$ group elements take the form

$$g = \begin{pmatrix} \frac{1}{c(e_1 - e_3)} & -\frac{e_1}{c(e_1 - e_3)} \\ c & -ce_2 \end{pmatrix}. \quad (98)$$

For these intersections the expressions for the Casimir functions are

$$\mathcal{H} : \quad k_2^2 u_2^2 + u_3^2 = \frac{e_1 - e_0}{e_1 - e_3}, \quad (99)$$

$$\mathcal{N} : \quad -k_2^2 u_1^2 + k_1^2 u_3^2 = \frac{e_2 - e_0}{e_1 - e_3}. \quad (100)$$

The surface \mathcal{H} has the same expression as (61) as it should be since we are working with the situation 1 of table 2, which corresponds to an elliptic cylinder.

- Simple pendulum with real time and Hamiltonian \mathcal{N} : Consider the momentum map (75)

$$u_1 \equiv \frac{k_1}{k_2} \sqrt{\frac{e_1 - e_0}{e_1 - e_3}} \frac{p}{2}, \quad u_2 \equiv \frac{1}{k_2} \sqrt{\frac{e_1 - e_0}{e_1 - e_3}} \sin\left(\frac{\theta}{2}\right), \quad u_3 \equiv \sqrt{\frac{e_1 - e_0}{e_1 - e_3}} \cos\left(\frac{\theta}{2}\right).$$

Clearly the Casimir \mathcal{H} is automatically satisfied whereas the Casimir

$$\mathcal{N} : \left(\frac{p}{2}\right)^2 + \sin^2\left(\frac{\theta}{2}\right) = \frac{1}{m^2}. \quad (101)$$

For values of $e_0 < e_2$, the quotient $1/m^2 < 1$ and therefore \mathcal{N} represents the Hamiltonian for the simple pendulum in oscillatory motion whereas for $e_0 > e_2$, $1/m^2 > 1$ and \mathcal{N} represents the Hamiltonian for the simple pendulum in circulating motion (40). For the limiting case $e_0 = e_2$, $1/m^2 = 1$ and we obtain the asymptotical motion.

As expected, in this case the two dimensional Lie-Poisson bracket coincides with (80) and therefore the Newton equation of motion is given by (81).

- Simple pendulum with imaginary time and Hamiltonian \mathcal{N} : Consider the momentum map (82)

$$u_1 \equiv i \frac{k_1}{k_2} \sqrt{\frac{e_1 - e_0}{e_1 - e_3}} \frac{\mathbb{P}}{2}, \quad u_2 \equiv \frac{1}{k_2} \sqrt{\frac{e_1 - e_0}{e_1 - e_3}} \cos\left(\frac{\theta'}{2}\right), \quad u_3 \equiv \sqrt{\frac{e_1 - e_0}{e_1 - e_3}} \sin\left(\frac{\theta'}{2}\right). \quad (102)$$

Under this map the Casimir \mathcal{H} is automatically satisfied whereas the Casimir \mathcal{N} becomes

$$\mathcal{N} : \left(\frac{\mathbb{P}}{2}\right)^2 + \sin^2\left(\frac{\theta'}{2}\right) = -\frac{m_c^2}{m^2}, \quad (103)$$

which is precisely the Hamiltonian of simple pendulum with imaginary time (83). Because we are using the same cotangent space (61) and (99), the rest of physical quantities such as the two dimensional Lie-Poisson bracket and the Newton equation of motion coincide with the ones mentioned below equation (83).

Following the previous cases, next natural situation is the one that maps the rigid body system to a cotangent space \mathcal{N} , with Hamiltonian \mathcal{H} . By inspection of Casimir (100), this can be achieved introducing a momentum map with a purely imaginary coordinate.

- Circulating pendulum with real time, imaginary coordinate and Hamiltonian \mathcal{H} : Consider the momentum map

$$u_1 \equiv \frac{i}{k_2} \sqrt{\frac{e_2 - e_0}{e_1 - e_3}} \cos\left(\frac{\theta}{2}\right), \quad u_2 \equiv \frac{1}{k_1 k_2} \sqrt{\frac{e_2 - e_0}{e_1 - e_3}} \frac{p}{2}, \quad u_3 \equiv \frac{1}{k_1} \sqrt{\frac{e_2 - e_0}{e_1 - e_3}} \sin\left(\frac{\theta}{2}\right). \quad (104)$$

Here we are assuming $e_2 - e_0 > 0$ (situation 7 in table 3).

Under this map the Casimir \mathcal{N} is satisfied, while the Hamiltonian \mathcal{H} has the following expression

$$\mathcal{H} : \left(\frac{p}{2}\right)^2 + \sin^2\left(\frac{\theta}{2}\right) = -\frac{m^2}{m_c^2}. \quad (105)$$

For values $e_2 - e_0 > 0$ the quotient $1 < -m^2/m_c^2 < \infty$ (see table 1) and we have a simple pendulum in circulating motion. Regarding the two dimensional Lie-Poisson bracket it has the following expression

$$\{f, g\}_{\mathcal{N}} = 8i \frac{(e_1 - e_2)(e_2 - e_3)}{\sqrt{(e_2 - e_0)(e_1 - e_3)}} \left(\frac{\partial f}{\partial \theta} \frac{\partial g}{\partial p} - \frac{\partial f}{\partial p} \frac{\partial g}{\partial \theta} \right), \quad (106)$$

whereas the Newton equation of motion reads

$$\frac{d^2\theta}{d\tau^2} = 16 \frac{(e_1 - e_2)^2(e_2 - e_3)^2}{(e_2 - e_0)(e_1 - e_3)} \sin \theta. \quad (107)$$

As the analogous physical situation in section 4.2, the extra minus sign that appears in the Newton equation (107) is due to the complex nature of the map (104). As for the case $e_0 > e_2$, we can go through it but the physical result will be the same, we only get the circulating movements of the pendulum.

- Circulating pendulum with imaginary time, imaginary coordinate and Hamiltonian \mathcal{H} : Consider the momentum map in which we assume $e_2 > e_0$

$$u_1 \equiv \frac{i}{k_2} \sqrt{\frac{e_2 - e_0}{e_1 - e_3}} \sin\left(\frac{\theta'}{2}\right), \quad u_2 \equiv \frac{i}{k_1 k_2} \sqrt{\frac{e_2 - e_0}{e_1 - e_3}} \frac{\mathbb{P}}{2}, \quad u_3 \equiv \frac{1}{k_1} \sqrt{\frac{e_2 - e_0}{e_1 - e_3}} \cos\left(\frac{\theta'}{2}\right). \quad (108)$$

Under this map the Casimir \mathcal{N} is satisfied, while the Hamiltonian \mathcal{H} has the following expression

$$\mathcal{H} : \left(\frac{\mathbb{P}}{2}\right)^2 + \sin^2\left(\frac{\theta'}{2}\right) = \frac{1}{m_c^2}. \quad (109)$$

It is clear that $-\infty < 1/m_c^2 < 0$ and therefore as expected we only have circulating motions.

For completeness, the two dimensional Lie-Poisson bracket is

$$\{f, g\}_{\mathcal{N}} = -8 \frac{(e_1 - e_2)(e_2 - e_3)}{\sqrt{(e_2 - e_0)(e_1 - e_3)}} \left(\frac{\partial f}{\partial \theta} \frac{\partial g}{\partial \mathbb{P}} - \frac{\partial f}{\partial \mathbb{P}} \frac{\partial g}{\partial \theta} \right), \quad (110)$$

whereas the equation of motion reads

$$\frac{d^2\theta}{d\tau^2} = -16 \frac{(e_1 - e_2)^2(e_2 - e_3)^2}{(e_2 - e_0)(e_1 - e_3)} \sin \theta. \quad (111)$$

Notice again the extra minus sign in (111) due to complex nature of the map (108).

5. The pendulum from the extended rigid body ($c \neq 0$ and $d = 0$)

Finally let us analyze the second general set of $SL(2, \mathbb{R})$ transformations. Regarding the conditions (55) the second one becomes modified to $ce_i = 0$. Since in this case $c \neq 0$ then necessarily $e_i = 0$. Even more, because we are restricted to the interval $\kappa \in (0, \pi/3)$ the only possibility is to have $e_2 = 0$ and because the restrictions (9) we also have $e_1 = -e_3 = \sqrt{3}/2$. We conclude that the conditions (55) can be satisfied only in two situations. In both of them $e_2 = 0$ and either $ae_1 + b = 0$ or $ae_3 + b = 0$. Due to the relation between e_1 and e_3 these two situations correspond to a transformation (27) with different sign of the coefficient a . So without losing generality we can restrict ourselves to the case $a > 0$ and analyze one of the situations. The second one can be obtained from the same formulas by changing the sign of a . In summary the conditions (9) become

$$ae_1 + b = 0, \quad e_2 = 0, \quad (112)$$

and a generic $SL(2, \mathbb{R})$ element has the form

$$g = \begin{pmatrix} \frac{1}{ce_1} & -\frac{1}{c} \\ c & 0 \end{pmatrix}. \quad (113)$$

Notice that this transformation can be obtained from (98) modulo a factor of $1/2$ in the first arrow of the matrix, which does not change the geometry of the Casimir surface \mathcal{H} and therefore (98) corresponds to the $SL(2, \mathbb{R})$ transformation that takes the original Casimir surfaces to an elliptic and a hyperbolic cylinders. Notice that for $e_1 = -e_3$ and $e_2 = 0$, the quotients (19) become equal $k_1^2 = k_2^2 = 1/2$.

It is clear that we do not have to developed this case further, since we can obtain it from a limiting case of the ones previously studied. Here we have two situations again, either $e_0 < 0$ (situation 1-7 of subsection 4.3) or $e_0 > 0$ (situation 1-6 of subsection 4.3).

6. Conclusions

In this paper we have revisited the relation between the extended rigid body and the simple pendulum with the aim to give an exhaustive list of all different ways in which the relation takes place. We started in section 2 reviewing the basics of the rigid body system in its two parameters formulation. The first parameter e_0 is related to the quotient E/L^2 where E is the energy of the motion and L^2 is the square of the magnitude of angular momentum. The second parameter κ codifies the values of the three moments of inertia. We work in this formulation of the rigid body because it allows us to have a good control on the different geometries of the two Casimir functions of the system [37].

The original construction to establish the relation between the extended rigid body and the pendulum was discussed by Holm and Marsden [33] and uses the $SL(2, \mathbb{R})$ symmetry of the Euler equations to find linear combinations of the two Casimir functions and transform them to new ones, denoted in this paper as \mathcal{H} and \mathcal{N} . For one specific class of $SL(2, \mathbb{R})$ transformations, both Casimirs have the geometry of an elliptic cylinder, this case corresponds to the extended rigid body with $ISO(2)$ Lie algebra. By a proper change of coordinates, or momentum map, and taking one of the cylinders as the cotangent space and the another one as the Hamiltonian, it is possible to obtain both the two dimensional Hamiltonian of the simple pendulum and its canonical equations of motion, even more, taking different values for the principal moments of inertia allows to get the different solutions of the simple pendulum: oscillatory, circulating and critical. Our present work revisits the construction proposed by Holm and Marsden in the two parameters formulation and, since we are working with a bi-

hamiltonian system, we give the momentum maps for the two different physical situations, i.e. when \mathcal{N} is the cotangent space and \mathcal{H} is the Hamiltonian and the situation where we invert the role of the Casimirs, \mathcal{H} as the cotangent space and \mathcal{N} as the Hamiltonian. This exercise allows us to understand in a precise way what kind of movements in the rigid body are mapped to certain type of movements of the simple pendulum. Specifically, we show that movements in the rigid body, for which $e_2 < e_0$, are mapped to oscillatory movements of the pendulum if \mathcal{H} is the Hamiltonian, but are mapped to circulating movements of the pendulum if \mathcal{N} is the Hamiltonian instead. Something similar occurs for movements with $e_2 > e_0$.

Going one step beyond and using the whole $SL(2, \mathbb{R})$ transformations of the Euler equations, in this paper we study all different cases in which there is a relation between the solutions of the extended rigid body and the ones of the simple pendulum or at least part of it. As a result, we have found that if we keep the geometry of one of the Casimirs an elliptic cylinder and we consider the other Casimir a hyperbolic cylinder, it is also possible to get the simple pendulum. To be specific, if \mathcal{H} represents the elliptic cylinder and \mathcal{N} represents the hyperbolic cylinder then we have again two situations: i) If \mathcal{H} is the cotangent space and \mathcal{N} is the Hamiltonian we can provide a momentum map that gives origin to the whole movements of the pendulum; this case also corresponds to an extended rigid body with Lie algebra $ISO(2)$. ii) If instead \mathcal{H} is the Hamiltonian and \mathcal{N} is the cotangent space, then we can provide a momentum map considering one of the coordinates as purely imaginary in such a way that we get the Hamiltonian of the pendulum, although the energies of the system correspond only to the circulating movements and not the oscillatory ones; this case corresponds to the extended rigid body with Lie algebra $ISO(1, 1)$. To the best of our knowledge this is a physical situation not previously discussed in the literature. In every case we also give the momentum map that relates the extended rigid body to the simple pendulum with imaginary time.

As for future work, because the analysis performed in this paper has been established only classically it would be interesting to extend the construction

to the quantum framework. We expect this analysis could produce interesting relations between Lame differential equation, which governs the quantum behaviour of the rigid body, and the Mathieu differential equation, which governs the quantum behaviour of the simple pendulum. A second possible direction of research is to investigate whether or not the dynamics of the pendulum could be used also to implement one-qubit quantum gates as the rigid body does [35].

Acknowledgments

The work of M. de la C. and N. G. is supported by the PhD scholarship program of the Universidad Autónoma Metropolitana. The work of R. L. is partially supported from CONACyT Grant No. 237351 “Implicaciones físicas de la estructura del espacio-tiempo”.

References

- [1] N. C. Abel, *Recherches sur les fonctions elliptiques*, *Journ. fur Math.* 2 (1827) 101–181 (1827).
- [2] C. G. J. Jacobi, *Demonstratio theorematis ad theoriam functionum ellipticarum spectantis*, *Astronomische Nachrichten* 6 (1827) 133 (1827).
- [3] C. G. J. Jacobi, *Fundamenta Nova Theoriae Functionum Ellipticarum*, 1829 (1829).
- [4] E. T. Whittaker, *A treatise on the Analytical Dynamics of particles and Rigid Motion*, 1917 (1917).
- [5] P. Du Val, *Elliptic Functions and Elliptic Curves*, 1973 (1973).
- [6] S. Lang, *Elliptic Functions*, 1973 (1973).
- [7] D. F. Lawden, *Elliptic Functions and Applications*, 1989 (1989).

- [8] H. McKean, V. Moll, *Elliptic Curves: Function Theory, Geometry, Arithmetic*, 1999 (1999).
- [9] J. V. Armitage, W. F. Eberlein, *Elliptic Functions*, 2006 (2006).
- [10] A. Beléndez, C. Pascual, D. I. Méndez, T. Beléndez, C. Neipp, Exact solution for the nonlinear pendulum, *Rev. Bras. Ensino Fís.* 29 (2007) 645–648 (2007).
- [11] K. Ochs, A comprehensive analytical solution of the nonlinear pendulum, *Eur. J. Phys.* 32 (2011) 479–490 (2011). [doi:doi:10.1088/0143-0807/32/2/019](https://doi.org/10.1088/0143-0807/32/2/019).
- [12] R. Linares, Duality symmetries behind solutions of the classical simple pendulum, *Rev. Mex. Fís. E* 64 (2018) 205–221 (2018). [arXiv:1601.07891](https://arxiv.org/abs/1601.07891).
- [13] E. U. Condon, The physical pendulum in quantum mechanics, *Phys. Rev.* 31 (1928) 891–894 (May 1928). [doi:10.1103/PhysRev.31.891](https://doi.org/10.1103/PhysRev.31.891).
- [14] T. Pradhan, A. V. Khare, Plane pendulum in quantum mechanics, *American Journal of Physics* 41 (1) (1973) 59–66 (1973). [doi:10.1119/1.1987121](https://doi.org/10.1119/1.1987121).
- [15] R. Aldrovandi, P. L. Ferreira, Quantum pendulum, *American Journal of Physics* 48 (8) (1980) 660–664 (1980). [doi:10.1119/1.12332](https://doi.org/10.1119/1.12332).
- [16] L. Euler, Du mouvement de rotation des corps solides autour d'un axe variable, *Mémoires de l'académie des sciences de Berlin* 14 (1758) 154–193 (1758).
- [17] L. Poinsot, *Theorie Nouvelle de la Rotation des Corps*, Bachelier, Paris, 1834 (1834).
- [18] L. D. Landau, E. M. Lifschitz, *Mechanics*, Vol. 1 of *Course of Theoretical Physics*, Pergamon Press, 1956 (1956).

- [19] J. E. Marsden, T. S. Ratiu, *Introduction to Mechanics and Symmetry. A Basic Exposition of Classical Mechanical Systems*, 1994 (1994).
- [20] E. Piña, *Dinámica de Rotaciones*, Colección CBI, Universidad Autónoma Metropolitana, México, 1996 (1996).
- [21] D. D. Holm, *Geometric Mechanics I: Dynamics and Symmetry*, World Scientific: Imperial College Press, Singapore, 2011 (2011).
- [22] H. A. Kramers, G. P. Ittmann, *Zur Quantelung des asymmetrischen Kreisels*, *Zs. f. Phys.* 53 (1929) 553 (1929).
- [23] G. W. King, *The asymmetric rotor. vi. calculation of higher energy levels by means of the correspondence principle*, *The Journal of Chemical Physics* 15 (11) (1947) 820–830 (1947). [doi:
http://dx.doi.org/10.1063/1.1746344](http://dx.doi.org/10.1063/1.1746344).
- [24] R. D. Spence, *Angular Momentum in spherico-conal coordinates*, *Am. J. Phys.* 27 (1959) 329 (1959).
- [25] I. Lukac, A. Smorodinskii, *The wave functions of an asymmetric top*, *Soviet Phys. JETP* 30 (1970) 728–730 (1970).
- [26] J. Patera, P. Winternitz, *A new basis for the representation of the rotation group. Lamé and Heun Polinomials*, *Journal of Mathematical Physics* 14 (1973) 1130 (1973).
- [27] E. Piña, *Some properties of the spectra of asymmetric molecules*, *Journal of Molecular Structure: {THEOCHEM}* 493 (13) (1999) 159 – 170 (1999).
- [28] M. T. Valdés, E. Piña, *The rotational spectra of the most asymmetric molecules*, *Rev. Mex. Fis.* 52 (2006) 220–229 (2006).
- [29] R. Méndez-Fragoso, E. Ley-Koo, *Rotations of Asymmetric Molecules and the Hydrogen Atom*, *Advances in Quantum Chemistry* 62 (2011) 137–213 (2011).

[30] R. Méndez-Fragoso, E. Ley-Koo, Chapter six - angular momentum theory in bases of lam spheroidal harmonics, in: J. R. Sabin, R. Cabrera-Trujillo (Eds.), Concepts of Mathematical Physics in Chemistry: A Tribute to Frank E. Harris - Part A, Vol. 71 of Advances in Quantum Chemistry, Academic Press, 2015, pp. 115 – 152 (2015). [doi:
http://dx.doi.org/10.1016/bs.aiq.2015.02.003](http://dx.doi.org/10.1016/bs.aiq.2015.02.003).

[31] Y. Nambu, Generalized Hamiltonian dynamics, *Phys. Rev. D* 7 (1973) 2405–2412 (1973). [doi:10.1103/PhysRevD.7.2405](https://doi.org/10.1103/PhysRevD.7.2405).

[32] A. Deprit, Free rotation of a rigid body studied in the phase plane, *American Journal of Physics* 35 (5) (1967) 424–428 (1967). [doi:10.1119/1.1974113](https://doi.org/10.1119/1.1974113).

[33] D. D. Holm, J. E. Marsden, The Rotor and the Pendulum, *Symplectic geometry and mathematical physics*, Progr. Math., 99, Birkhauser Boston, Boston, MA. (1991) 189–203 (1991).

[34] R. Montgomery, How much does the rigid body rotate? a berry’s phase from the 18th century, *American Journal of Physics* 59 (1991) 394–398 (1991).

[35] L. Van Damme, D. Leiner, P. Mardesic, S. J. Glaser, D. Sugny, Linking the rotation of a rigid body to the schrödinger equation: The quantum tennis racket effect and beyond, *Scientific Reports* 7-3998 (2017) 1–8 (2017).

[36] T. Iwai, D. Tarama, Classical and quantum dynamics for an extended free rigid body, *Differential Geometry and its Applications* 28 (5) (2010) 501 – 517 (2010).

[37] M. de la Cruz, N. Gaspar, L. Jiménez-Lara, R. Linares, Classification of the classical $SL(2, \mathbb{R})$ gauge transformations in the rigid body, *Annals Phys.* 379 (2017) 112–130 (2017). [arXiv:1612.08824](https://arxiv.org/abs/1612.08824), [doi:10.1016/j.aop.2017.02.016](https://doi.org/10.1016/j.aop.2017.02.016).

- [38] A. J. Brizard, A primer on elliptic functions with applications in classical mechanics, *Eur. J. Phys.* 30 (2009) 729–750 (2009). [arXiv:0711.4064](https://arxiv.org/abs/0711.4064), [doi:10.1088/0143-0807/30/4/007](https://doi.org/10.1088/0143-0807/30/4/007).
- [39] P. Appell, *Principes de la théorie des fonctions elliptiques et applications*, 1897 (1897).
- [40] H. Von Helmholtz, O. Krigar-Menzel, *Die Dynamik Discreter Massenpunkte*, 1898 (1898).
- [41] P. Appell, Sur une interprtation des valeurs imaginaires du temps en Mcanique, *Comptes Rendus Hebdomadaires des Scances de l'Acadmie des Sciences* 87 (1878).
- [42] D. David, D. D. Holm, Multiple lie-poisson structures, reductions, and geometric phases for the maxwell-bloch travelling wave equations, *Journal of Nonlinear Science* 2 (2) (1992) 241–262 (1992). [doi:10.1007/BF02429857](https://doi.org/10.1007/BF02429857).